

Article

# 3D Viscoplastic Finite Element Modeling of Dislocation Generation in a Large Size Si Ingot of the Directional Solidification Stage

Maohua Lin <sup>1,\*</sup> , Xinjiang Wu <sup>2</sup>, Xinqin Liao <sup>3</sup> , Min Shi <sup>1</sup>, Disheng Ou <sup>4</sup> and Chi-Tay Tsai <sup>1,\*</sup><sup>1</sup> Department of Ocean and Mechanical Engineering, Florida Atlantic University, Boca Raton, FL 33431, USA<sup>2</sup> School of Engineering, Fujian Jiangxia University, Fuzhou 350108, China<sup>3</sup> School of Electrical and Electronic Engineering, Nanyang Technological University, 50 Nanyang Avenue, Singapore 639798, Singapore<sup>4</sup> Department of Material Science and Engineering, Guangxi Technology University, Liuzhou 345006, China

\* Correspondence: mlin2014@fau.edu (M.L.); tsaict@fau.edu (C.-T.T.)

Received: 10 July 2019; Accepted: 21 August 2019; Published: 29 August 2019



**Abstract:** Growing very large size silicon ingots with low dislocation density is a critical issue for the photovoltaic industry to reduce the production cost of the high-efficiency solar cell for affordable green energy. The thermal stresses, which are produced as the result of the non-uniform temperature field, would generate dislocation in the ingot. This is a complicated thermal viscoplasticity process during the cooling process of crystal growth. A nonlinear three-dimensional transient formulation derived from the Hassen-Sumino model (HAS) was applied to predict the number of dislocation densities, which couples the macroscopic viscoplastic deformation with the microscopic dislocation dynamics. A typical cooling process during the growth of very large size (G5 size: 0.84 m × 0.84 m × 0.3 m) Si ingot is used as an example to validate the developed HAS model and the results are compared with those obtained from qualitatively critical resolved shear stress model (CRSS). The result demonstrates that this finite element model not only predicts a similar pattern of dislocation generation with the CRSS model but also anticipate the dislocation density quantity generated in the Si ingot. A modified cooling process is also employed to study the effect of the cooling process on the generation of the dislocation. It clearly shows that dislocation density is drastically decreased by modifying the cooling process. The results obtained from this model can provide valuable information for engineers to design a better cooling process for reducing the dislocation density produced in the Si ingot under the crystal growth process.

**Keywords:** hassen-sumino model; CRSS model; dislocation density; a cooling process; directly solidification process

## 1. Introduction

Si crystal is the primary materials for solar cell for green energy applications [1]. Typically, high dislocation density generated in Si crystal will decrease the photoelectric conversion efficiency, reliability and lifetime of the solar cells [2,3]. To get a lower dislocation density Si ingot at a lower cost, the effects from crystal growth process on the dislocation generation have to be understood and the dislocation density produced in the crystal can be anticipated. However, the dislocation generation process of Si crystal is a complex thermal viscoplasticity process. Many works have been done to predict the generation of dislocation density in the crystals [4,5]. The first model to predict dislocation generation during crystal growth is called the critical resolved shear stress model (CRSS) proposed by Jordan [6,7], where the dislocation generation in the crystal is assumed to be correlated to the excessive resolved shear stress during the crystal growth process. This model can provide a qualitative

prediction of dislocation density distribution cumulated in the ingot even though the actual quantity of dislocation density cumulated in the silicon ingot cannot be directly predicted. Another numerical model was first developed by Tsai [8] based on the Hassen-Sumino model (HAS) model [9]. HAS model couples the microscopic dislocation dynamics with the macroscopic viscoplastic deformation and it can directly predict the actual dislocation density generation during crystal growth. Since then, HAS model has been widely employed to calculate the dislocation density quantification of Si, GaAs and InP crystal from various crystal growth processes [10–12]. However, their works were based on the quasi-steady-state two-dimensional model. Furthermore, most crystals being investigated are axisymmetric crystal in nature [12–14]. Chen [15,16] has developed a three dimensional finite volume algorithm for the prediction of dislocation density generation in a non-axisymmetric silicon ingot. However, the finite volume method is not flexible in modelling complex geometry and boundary conditions of crystal growth process [17]. Therefore, in our modelling of very large 0.84 m × 0.84 m × 0.3 m block ingots grown by directional solidification process, a three-dimensional transient finite element analysis (FEA) model is needed to predict the dislocation density in the non-axisymmetric crystal. One original and one modified cooling process [2,18] are employed to this developed transient model to predict the dislocation densities from the Si crystal. The results from the original cooling process will be compared with the results obtained from the CRSS model to demonstrate the validity of this developed model. It will be furthermore compared with the results from the modified cooling process to check out the initial cooling process. This developed finite element model is expected to provide a meaningful tool for engineers and scientists to design crystal growth and cooling processes for growing large size low dislocation density crystals.

## 2. Three Dimensional Viscoplastic Finite Element Model

The finite element model is developed from the Hassen-Sumino (HAS) model. In the Hassen-Sumino model [2,9,19–21], the viscoplastic strain components  $\varepsilon_{ij}^c$ , the viscoplastic rate component  $\dot{\varepsilon}_{ij}^{pl}$ , and dislocation density multiplication rate  $\dot{N}_m$  are given as:

$$\varepsilon_{ij}^{pl} = \int_0^t \dot{\varepsilon}_{ij}^{pl} dt \quad (1)$$

$$\dot{\varepsilon}_{ij}^{pl} = \frac{1}{2} b k_0 N_m e^{(-Q/kT)} (\sqrt{J_2} - A \sqrt{N_m})^p \frac{S_{ij}}{\sqrt{J_2}} \quad (2)$$

$$\dot{N}_m = K k_0 N_m e^{(-Q/kT)} (\sqrt{J_2} - A \sqrt{N_m})^{p+\lambda} \quad (3)$$

$$J_2 = \frac{S_{ij} S_{ij}}{2}, \quad (4)$$

where  $k$  is the Boltzmann constant that is  $8.617 \times 10^{-5}$  eV·K,  $K$ ,  $k_0$  and  $\lambda$  are material constants of Si and given to be  $3.1 \times 10^{-4}$  m/N,  $8.6 \times 10^{-4}$  m<sup>2p+1</sup>N<sup>-ps-1</sup> and 1, respectively.  $N_m$  is mobile dislocation density,  $A$  (strain hardening coefficient) is  $4$  N·m<sup>-1</sup>,  $Q$  (activation energy) is 2.2 eV,  $p$  (the stress exponent) 1.1,  $b$  (Burgers vector of Si) is  $3.8 \times 10^{-10}$  m,  $S_{ij}$  is the deviatoric stress component, and  $\sqrt{J_2}$  indicates the equivalent stress.  $\dot{N}_m$  and  $\dot{\varepsilon}_{ij}^{pl}$  is set to zero when  $\sqrt{J_2} - A \sqrt{N_m} \leq 0$ .

Since the dislocation multiplication during the cooling stage is a transient process in nature, a nonlinear three dimensional model is made to get dislocation densities in the ingot. The model can be formulated as [22]:

$$[K]_n \{\Delta d\}_n = \{\Delta F\}_n \quad (5)$$

where

$$[K]_n = \int_V [B]^T [\hat{D}]_n [B] dV \quad (6)$$

and

$$\{\Delta F\}_n = \int_V [B]^T [\hat{D}]_n (\{\dot{\varepsilon}^c\}_n \Delta t_n + \{\Delta \varepsilon^{th}\}_n) dV \quad (7)$$

In Equations (5)–(7),  $\{\Delta d\}_n$  is the displacement,  $[B]$  is the matrix,  $\{\Delta \varepsilon^{th}\}_n$  is the thermal strain and  $\{\Delta F\}_n$  is the equivalent load in a  $\Delta t_n = t_{n+1} - t_n$ . The viscoplastic material matrix is given by:

$$[\hat{D}]_n = \left( [D]^{-1} + \theta \left[ \frac{\partial \dot{\varepsilon}^c}{\partial \sigma} \right]_n \Delta t_n \right)^{-1} \quad (8)$$

$[D]$  is the elastic material matrix. After calculating  $\{\Delta d\}_n$ , the displacement, residual stresses components and dislocation densities at time  $t_{n+1}$  can be calculated from:

$$\{d\}_{n+1} = \{d\}_n + \{\Delta d\}_n, \quad (9)$$

$$\{\sigma\}_{n+1} = \{\sigma\}_n + \{\Delta \sigma\}_n, \quad (10)$$

$$(N)_{n+1} = (N)_n + (\dot{N})_n \Delta t_n. \quad (11)$$

The initial dislocation density was assumed as  $1.0 \times 10^6 \text{ m}^{-2}$  in this paper.

### 3. Results and Discussions

One very large size Si ingot,  $0.84 \text{ m} \times 0.84 \text{ m} \times 0.3 \text{ m}$  is used to get the dislocation densities from the ingot during the cooling stage. One original and one modified cooling process during the growth of Si ingot are adopted to calculate the temperature field in the silicon crystal [2,18]. In the cooling process, the ingot top central temperature  $T_{c1}$  and the bottom central temperature  $T_{c2}$  are given in Figure 1 [2,18]. The temperature distribution in the silicon ingot is calculated by heat transfer module from commercial software COMSOL Multiphysics 5.2 (Burlington, COMSOL) [18]. The temperature distribution in the silicon caused by the cooling stage at different time steps as shown in Figure 2 are then coupled with the developed three-dimensional FEA model to get the dislocation densities in the silicon.

The temperature distributions caused by the cooling stage are shown in Figure 2. Figure 2a shows the initial temperature distribution of  $0.84 \text{ m} \times 0.84 \text{ m} \times 0.3 \text{ m}$  silicon ingot at the beginning of the original cooling process. The temperature distribution shows a four-fold symmetry in the x-y plane. The value gradually increases from 1350 K at the center of the bottom surface of ingot to 1694 K at the four corners of the top ingot surface. The temperature in the original process is higher than 1073 K. The excessive stress will lead to the multiplication of dislocations in the ductile silicon crystal, and then the crystal deformation and stress release. After the 200th, 400th, and 850th min of cooling, the value of the maximum temperature difference between the bottom and top ingot decreases to about 40 K, 32 K, and 7 K, respectively as shown in Figure 2b–d. Figure 3a shows the initial temperature distribution of  $0.84 \text{ m} \times 0.84 \text{ m} \times 0.3 \text{ m}$  silicon ingot at the beginning of the modified cooling process, where the temperature distribution is the same with Figure 2a from the original cooling process. After 200th, 400th, and 790th min (the minute is not consistent with Figure 1 of cooling, the value of the maximum temperature difference between the bottom and top ingot decreases to about 230 K, 31 K, and 7 K, respectively as shown in Figure 3b–d). Compared with the original cooling process, the temperature decrease in the modified cooling process is much smooth during the first 200 min, which will cause less generation of dislocation density in the modified cooling process theoretically.

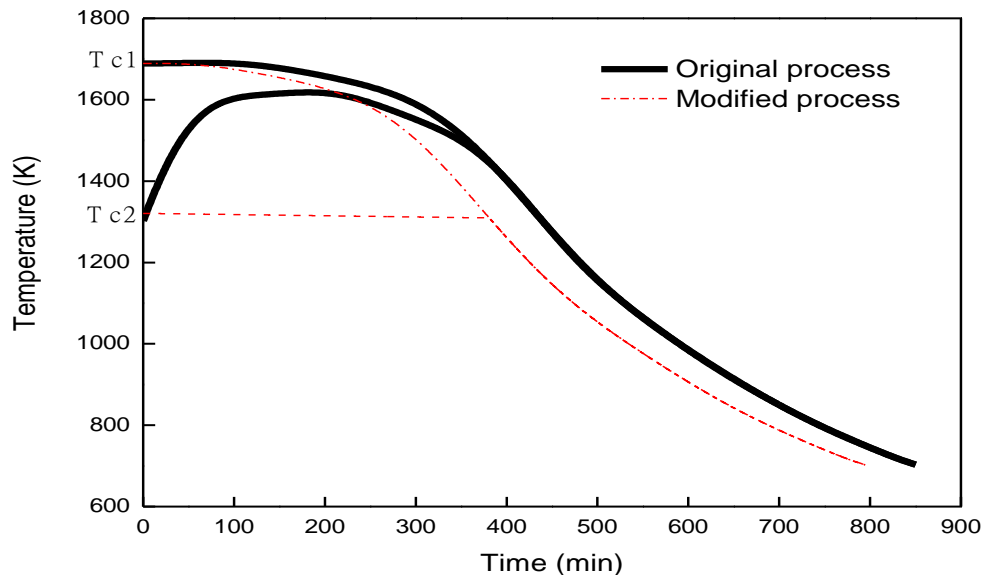


Figure 1. Temperature diagram (Tc1 and Tc2) with time under original and modified cooling process.

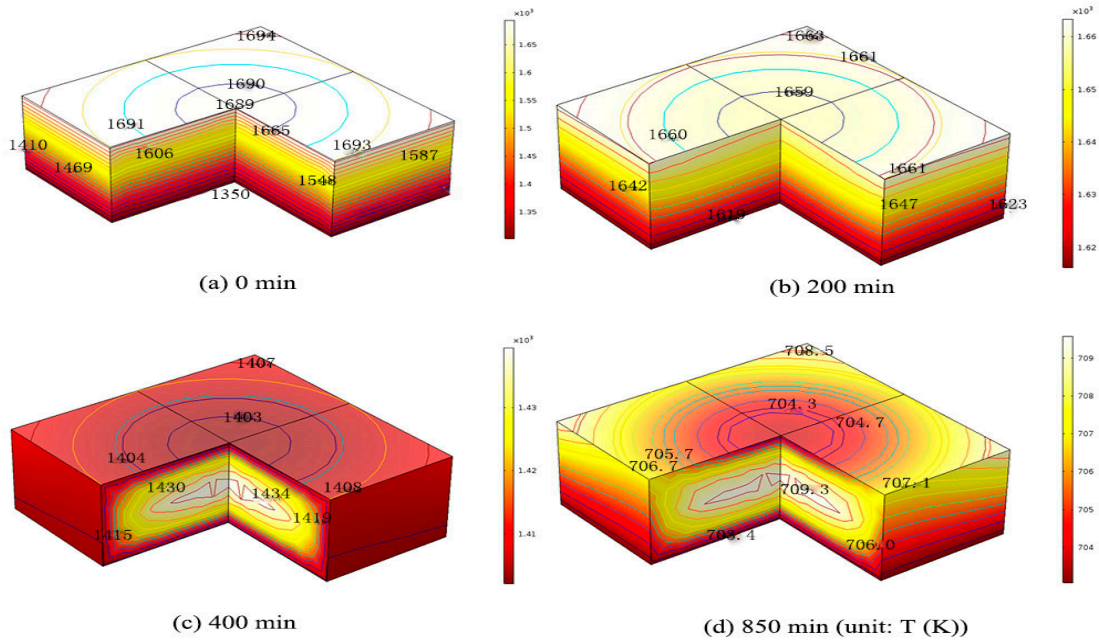
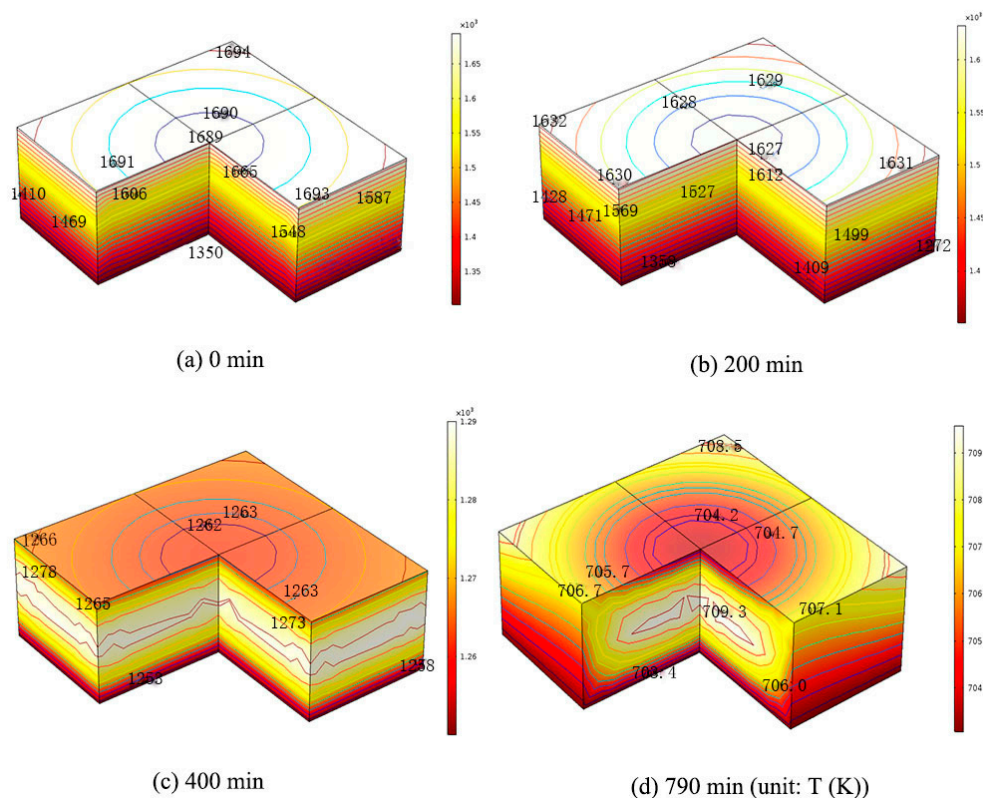


Figure 2. Temperature distribution of  $0.84\text{m} \times 0.84\text{m} \times 0.3\text{m}$  silicon ingot at (a) beginning (0 min), (b) 200 min, (c) 400 min, and (d) end of the original cooling process (850 min).



**Figure 3.** Temperature distribution of  $0.84 \text{ m} \times 0.84 \text{ m} \times 0.3 \text{ m}$  silicon ingot at (a) beginning (0 min), (b) 200 min, (c) 400 min, and (d) end of the modified cooling process (790 min).

The temperature field caused by the cooling process at different time steps as shown in Figure 2 are then coupled with the developed three-dimensional FEA model to calculate the dislocation densities from in the silicon. Figure 4 shows the final dislocation density distribution in the  $0.84 \text{ m} \times 0.84 \text{ m} \times 0.3 \text{ m}$  silicon ingot calculated by Hassen model. On the top surface as shown in Figure 4a, the red region has a higher dislocation density of about  $4.0 \times 10^8 \text{ m}^{-2}$ , while the lower dislocation density of about  $9.3 \times 10^7 \text{ m}^{-2}$  occurs near the edges of the top surface. Figure 4b shows final dislocation density variation on the middle surface ( $z = 0.15 \text{ m}$ ) of the ingot, where the blue region has a lower dislocation density of about  $5.0 \times 10^7 \text{ m}^{-2}$ , while the largest dislocation density of about  $3.5 \times 10^8 \text{ m}^{-2}$  occurs at the edges of the middle surface as shown in Figure 4b, c shows the final dislocation density variation on the bottom plane ( $z = 0 \text{ m}$ ) of the ingot during the original cooling process, where the red region has a higher dislocation density of about  $3.7 \times 10^8 \text{ m}^{-2}$ , while the lower dislocation density of about  $4.7 \times 10^7 \text{ m}^{-2}$  occurs near the edges of the bottom. The results are in good agreement with the reported experimental data [23].

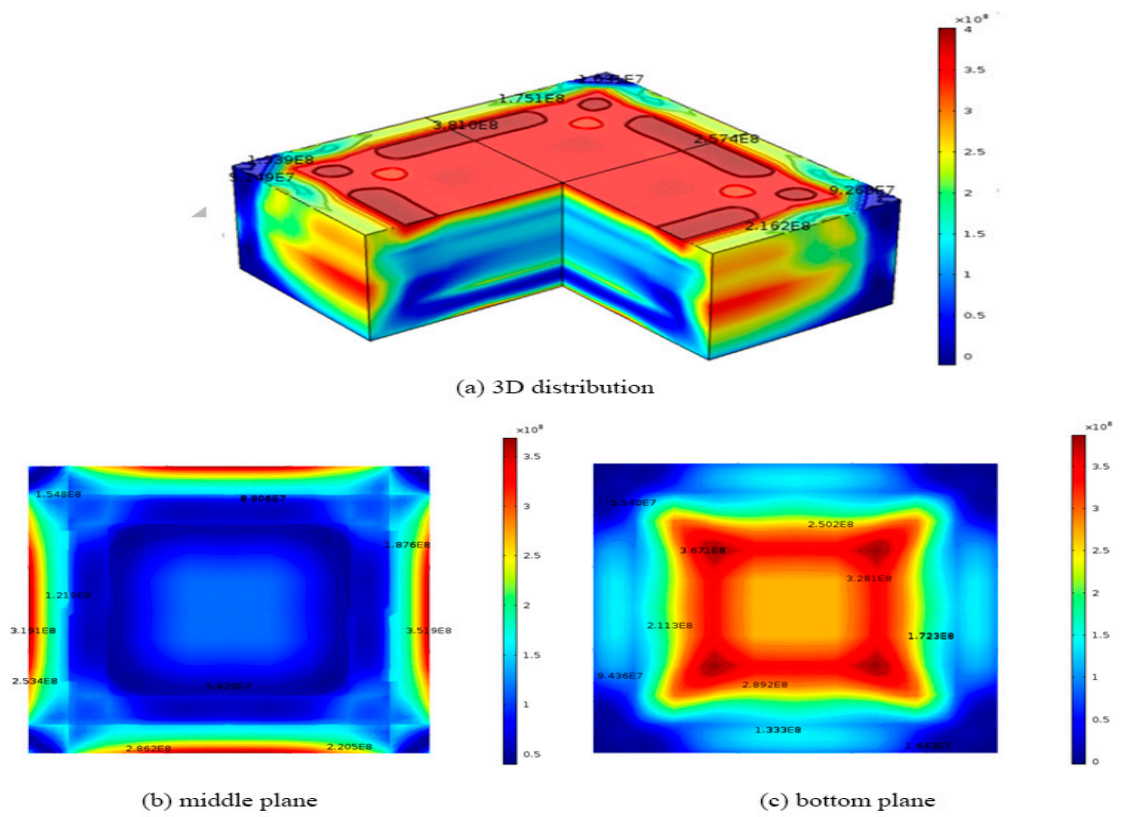
We also compared the results obtained from our HAS model with those derived from the CRSS model [18]. In order to obtain a representative quantity of dislocation density, the CRSS model is derived by multiplying the excessive elastic stresses by a dislocation multiplication factor derived from HAS model [18]. Since the CRSS model does not consider the plastics deformation during the cooling process, the stress relaxation will not occur and the calculated dislocation density will be overestimated. However, the results from CRSS model can still predict the correct trend and qualitative distribution of dislocation density. The dislocation densities are solved by the CRSS model generated by the original cooling process in a  $0.84 \text{ m} \times 0.84 \text{ m} \times 0.3 \text{ m}$  silicon ingot. in Figure 5, the maximum dislocation density is about  $3.1 \times 10^{10} \text{ m}^{-2}$  on the top surface of the silicon, while the minimum dislocation density is about  $1.2 \times 10^9 \text{ m}^{-2}$  on the bottom surface. On the top surface, the red region has a higher dislocation density of about  $3.1 \times 10^{10} \text{ m}^{-2}$ , while the lower dislocation density of about  $1.1 \times 10^{10} \text{ m}^{-2}$  occurs near the edges of the top surface as shown in Figure 5a. Figure 5b shows final dislocation density variation on the middle surface ( $z = 0.15 \text{ m}$ ) of the ingot during the original cooling process, where the blue

region has a lower dislocation density of about  $3.8 \times 10^9 \text{ m}^{-2}$ , while the largest dislocation density of about  $1.4 \times 10^{10} \text{ m}^{-2}$  occurs at the edges of the middle surface as shown in Figure 5b. Figure 5c shows the final dislocation density variation on the bottom plane ( $z = 0 \text{ m}$ ) of the ingot during the original cooling process, where the red region has a higher dislocation density of about  $1.2 \times 10^{10} \text{ m}^{-2}$ , while the lower dislocation density of about  $1.2 \times 10^9 \text{ m}^{-2}$  occurs near the edges of the bottom surface as shown in Figure 5c. The results show that the distribution pattern of dislocation density obtained from both models is similar except the magnitude of dislocation densities obtained from the CRSS model is 100 times higher than those obtained from this developed model. The dislocation density distribution pattern from both models also shows a famous four-fold symmetry. These results are expected since the CRSS model assumes the dislocation density generated by the crystal is proportional to the excessive elastic stress, which does not consider the stress relaxation due to plastic deformation caused by dislocation multiplication. Therefore, its dislocation density based on the accumulation of excessive elastic stress will be much higher.

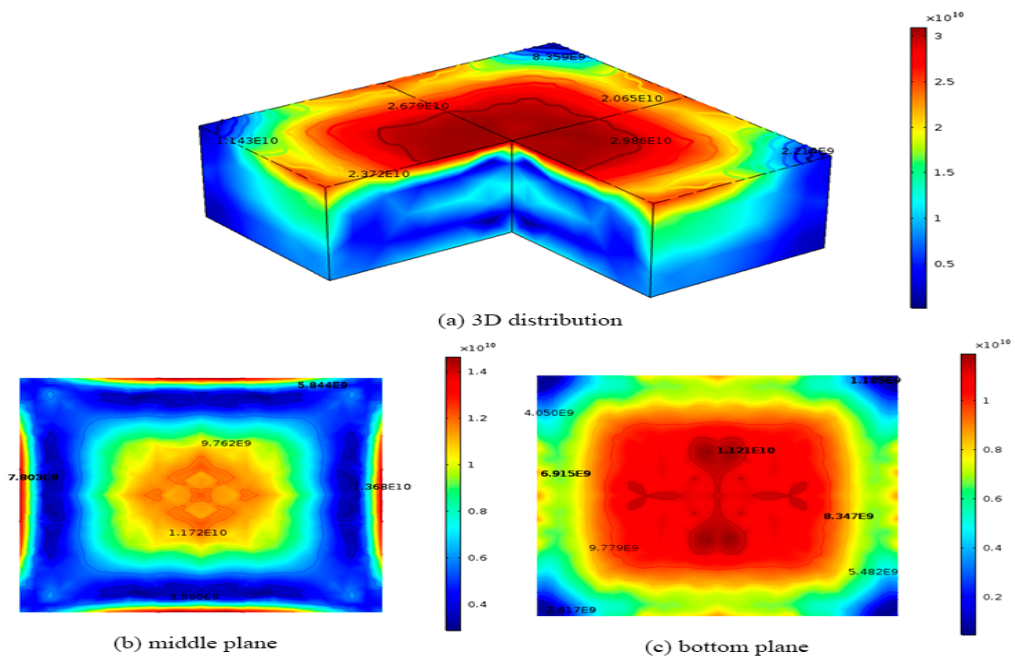
Figure 6 shows the final dislocation density distribution in  $0.84 \text{ m} \times 0.84 \text{ m} \times 0.3 \text{ m}$  silicon obtained from the developed model with the modified cooling process. The maximum dislocation density of about  $3.2 \times 10^8 \text{ m}^{-2}$  is on the top surface of the silicon and the minimum dislocation density is about  $1.4 \times 10^7 \text{ m}^{-2}$  on the bottom surface of the silicon ingot. On the top surface, the red region has a higher dislocation density of about  $3.2 \times 10^8 \text{ m}^{-2}$  as shown in Figure 6a, which is 20% lower than that in the original cooling process, while the lower dislocation density of about  $1.1 \times 10^7 \text{ m}^{-2}$  occurs near the edges of the top surface. Figure 6b shows final dislocation density variation on the middle surface ( $z = 0.15 \text{ m}$ ) of the ingot during the original cooling process, where the blue region has a lower dislocation density of about  $2.0 \times 10^7 \text{ m}^{-2}$ , while the largest dislocation density of about  $2.0 \times 10^8 \text{ m}^{-2}$  occurs at the edges of the middle surface as shown in Figure 6b, which is 42.9% lower than in the original cooling process. Figure 6c shows the final dislocation density variation on the bottom plane ( $z = 0 \text{ m}$ ) of the ingot during the original cooling process, where the red region has a higher dislocation density of about  $8.3 \times 10^7 \text{ m}^{-2}$ , which is 77% lower than in the original cooling process, while the lower dislocation density of about  $9.2 \times 10^6 \text{ m}^{-2}$  occurs near the edges of the bottom surface as shown in Figure 6c.

Figure 7 shows the final dislocation density distribution in the  $0.84 \times 0.84 \times 0.3 \text{ m}$  silicon ingot for CRSS model with modified cooling process. The maximum dislocation density is about  $1.6 \times 10^{10} \text{ m}^{-2}$  on the top surface of the silicon, which is 46.7% lower than that in original cooling process. The minimum dislocation density is about  $9.3 \times 10^7 \text{ m}^{-2}$  on the bottom surface of the silicon ingot. On the top surface, the red region has a higher dislocation density of about  $1.6 \times 10^{10} \text{ m}^{-2}$ , while the lower dislocation density of about  $1.1 \times 10^9 \text{ m}^{-2}$  occurs near the edges of the top surface as shown in Figure 7a, b shows final dislocation density variation on the middle surface ( $z = 0.15 \text{ m}$ ) of the ingot during the original cooling process, where the blue region has a lower dislocation density of about  $5.0 \times 10^8 \text{ m}^{-2}$ , while the largest dislocation density of about  $3.3 \times 10^9 \text{ m}^{-2}$  occurs at the edges of the middle surface as shown in Figure 7b, which is 76.4% lower than that in the original cooling process. Figure 7c shows the final dislocation density variation on the bottom plane ( $z = 0 \text{ m}$ ) of the ingot, where the red region has a higher dislocation density of about  $6.1 \times 10^8 \text{ m}^{-2}$ , which is 95% lower than in the original cooling process, while the lower dislocation density of about  $9.3 \times 10^7 \text{ m}^{-2}$  on the bottom surface as shown in Figure 7c.

From Figures 4–7, we can find that the distributions of dislocation density are almost similar as follows: Where the top and the bottom of the silicon hold the maximum dislocation density, while the four corners of the silicon hold the minimum dislocation density. However, the quantity in HAS model is much more accurate than that in the CRSS model. Also, the dislocation density and the scope of final dislocation density in CRSS model are quite higher than that in the HAS model as the stress does not release in CRSS model during the transient viscoplastic deform process. For the modified cooling process, the dislocation density is lower than that of the initial cooling stage both in the CRSS model and the HAS model. However, the HAS model can predict quantitatively and more accurate to be used in the cooling stage than the CRSS model.



**Figure 4.** Dislocation density distributions of 0.84 m × 0.84 m × 0.3 m ingot at the end of the cooling process obtained from Hassen model with the original cooling process (a) 3D distribution; (b) middle plane; (c) bottom plane.



**Figure 5.** Dislocation density distributions of 0.84 m × 0.84 m × 0.3 m ingot at the end of the cooling process obtained from the critical resolved shear stress model (CRSS) model with the original cooling process (a) 3D distribution; (b) middle plane; (c) bottom plane.

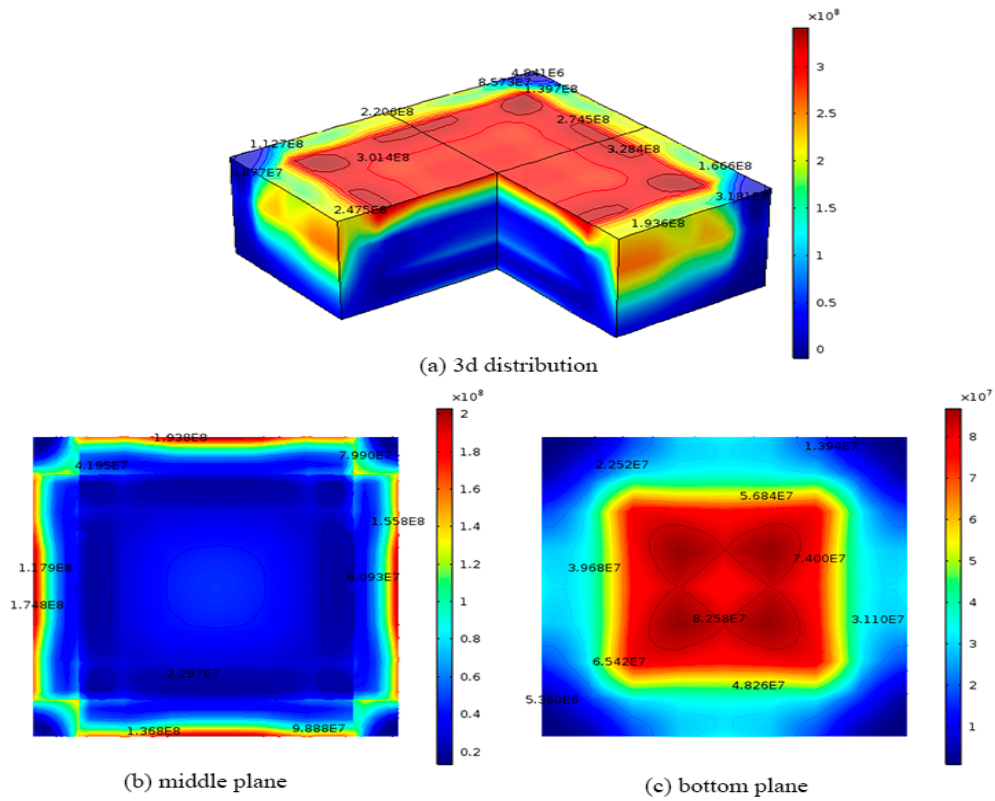


**Figure 6.** Dislocation density distributions of 0.84 m  $\times$  0.84 m  $\times$  0.3 m ingot at the end of the cooling process obtained from Hassen model with the modified cooling process (a) 3D distribution; (b) middle plane; (c) bottom plane.

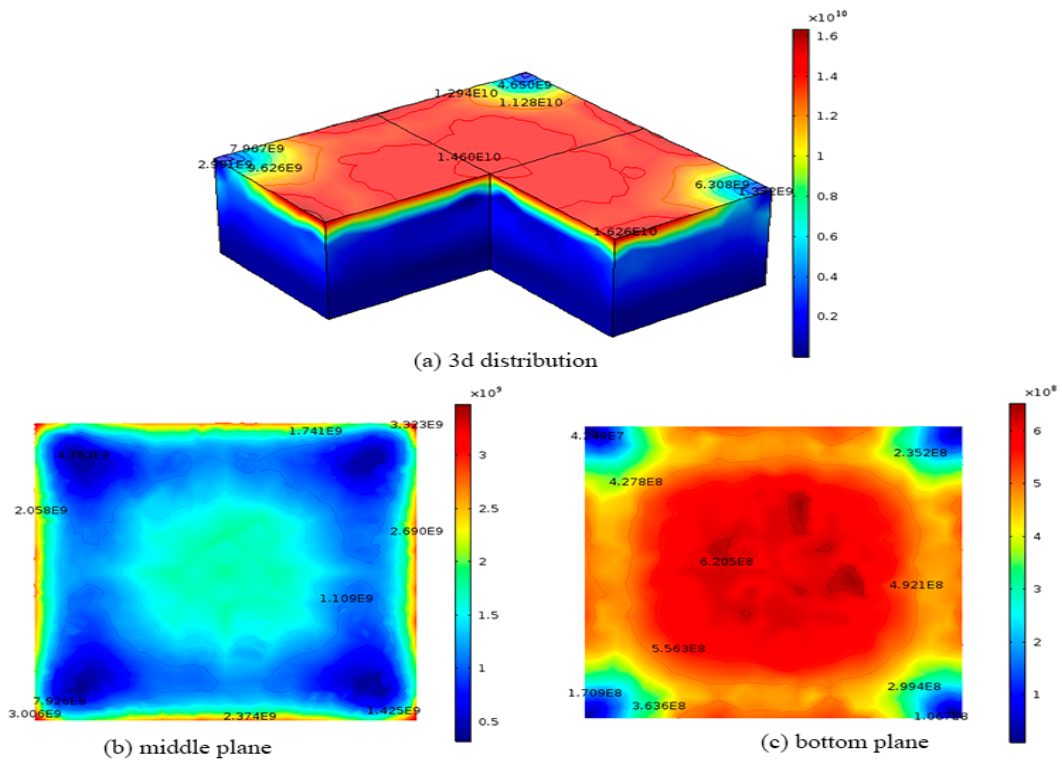


**Figure 7.** Dislocation density distributions of 0.84 m  $\times$  0.84 m  $\times$  0.3 m ingot at the end of the cooling process obtained from the CRSS model with the modified cooling process (a) 3D distribution; (b) middle plane; (c) bottom plane.

#### 4. Conclusions

A nonlinear three dimensional transient FEA model is successfully developed from the HAS constitutive model. The conventional CRSS model is used as a control group to compare with HAS model. The results obtained from both models show that the distribution of dislocation density is similar for both the original and modified cooling process. However, the magnitude of dislocation densities obtained from the HAS model is 100× lower than those obtained from the CRSS model. The maximum dislocation density obtained from the HAS model shows a reduction of 20% from original cooling process to modified cooling process, while the reduction is 46.7% from CRSS model. The reason that the HAS model predicts lower dislocation density and less dislocation reduction than the CRSS model is due to the fact that the CRSS model does not include the plastic deformations in its constitutive material model during numerical calculation. Therefore, the HAS model is a better model for predicting the quantity of dislocation generation during cooling process of crystal growth.

**Author Contributions:** Conceptualization, Formal analysis and Writing—Original draft, M.L. and C.-T.T.; Investigation and Visualization, X.W.; Formal analysis and Visualization, X.L., D.O.; Methodology, M.S.

**Funding:** This research received no external funding.

**Conflicts of Interest:** The authors declare no conflict of interests.

#### References

- Poullikkas, A.; Kourtis, G.; Hadjipaschalis, I. Parametric analysis for the installation of solar dish technologies in Mediterranean regions. *Renew. Sustain. Energy Rev.* **2010**, *14*, 2772–2783. [[CrossRef](#)]
- Zhou, N.; Lin, M.; Wan, M.; Zhou, L. Lowering dislocation density of directionally grown multicrystalline silicon ingots for solar cells by simplifying their post-solidification processes—A simulation approach. *J. Therm. Stress.* **2015**, *38*, 146–155. [[CrossRef](#)]
- Fang, H.S.; Wang, S.; Zhou, L.; Zhou, N.G.; Lin, M.H. Influence of furnace design on the thermal stress during directional solidification of multicrystalline silicon. *J. Cryst. Growth* **2012**, *346*, 5–11. [[CrossRef](#)]
- Yonenaga, I.; Sumino, K. Dislocation dynamics in the plastic deformation of silicon crystals I. Experiments. *Phys. Status Solidi A* **1978**, *50*, 685–693. [[CrossRef](#)]
- Suezawa, M.; Sumino, K.; Yonenaga, I. Dislocation dynamics in the plastic deformation of silicon crystals. II. Theoretical analysis of experimental results. *Phys. Status Solidi A* **1979**, *51*, 217–226. [[CrossRef](#)]
- Jordan, A.S.; Caruso, R.; Von Neida, A.R. A Thermoelastic analysis of dislocation generation in pulled GaAs crystals. *Bell Syst. Tech. J.* **1980**, *59*, 593–637. [[CrossRef](#)]
- Jordan, A.S.; Von Neida, A.R.; Caruso, R. The theoretical and experimental fundamentals of decreasing dislocations in melt grown GaAs and InP. *J. Cryst. Growth* **1986**, *79*, 243–262. [[CrossRef](#)]
- Dillon, O.W.; Tsai, C.T.; De Angelis, R.J. Dislocation dynamics during the growth of silicon ribbon. *J. Appl. Phys.* **1986**, *60*, 1784–1792. [[CrossRef](#)]
- Alexander, H.; Haasen, P. Dislocations and plastic flow in the diamond structure. In *Solid State Physics*; Elsevier: Amsterdam, The Netherlands, 1969; Volume 22, pp. 27–158. ISBN 978-0-12-607722-3.
- Tsai, C.T.; Dillon, O.W.; De Angelis, R.J. The constitutive equation for silicon and its use in crystal growth modeling. *J. Eng. Mater. Technol.* **1990**, *112*, 183. [[CrossRef](#)]
- Tsai, C.T.; Yao, M.W.; Chait, A. Prediction of dislocation generation during Bridgman growth of GaAs crystals. *J. Cryst. Growth* **1992**, *125*, 69–80. [[CrossRef](#)]
- Tsai, C.T.; Gulluoglu, A.N.; Hartley, C.S. A crystallographic methodology for modeling dislocation dynamics in GaAs crystals grown from melt. *J. Appl. Phys.* **1993**, *73*, 1650–1656. [[CrossRef](#)]
- Wang, Q.; Wu, G.; Liu, S.; Gan, Z.; Yang, B.; Pan, J. Simulation-based development of a new cylindrical-cavity microwave-plasma reactor for diamond-film synthesis. *Crystals* **2019**, *9*, 320. [[CrossRef](#)]
- Laiarinandrasana, L. Stress heterogeneity leading to void nucleation within spherulites for semi-crystalline polymers. *Crystals* **2019**, *9*, 298. [[CrossRef](#)]
- Chen, X.J.; Nakano, S.; Kakimoto, K. 3D numerical analysis of the influence of material property of a crucible on stress and dislocation in multicrystalline silicon for solar cells. *J. Cryst. Growth* **2011**, *318*, 259–264. [[CrossRef](#)]

16. Chen, X.J.; Nakano, S.; Liu, L.J.; Kakimoto, K. Study on thermal stress in a silicon ingot during a unidirectional solidification process. *J. Cryst. Growth* **2008**, *310*, 4330–4335. [[CrossRef](#)]
17. Nakano, S.; Chen, X.J.; Gao, B.; Kakimoto, K. Numerical analysis of cooling rate dependence on dislocation density in multicrystalline silicon for solar cells. *J. Cryst. Growth* **2011**, *318*, 280–282. [[CrossRef](#)]
18. Zhou, N.; Lin, M.; Zhou, L.; Hu, Q.; Fang, H.; Wang, S. A modified cooling process in directional solidification of multicrystalline silicon. *J. Cryst. Growth* **2013**, *381*, 22–26. [[CrossRef](#)]
19. Haasen, P. Zur plastischen Verformung von Germanium und InSb. *Zeitschrift Für Phys.* **1962**, *167*, 461–467. [[CrossRef](#)]
20. Lin, M.; Chen, Q.; Kang, Y.; Tsai, C. 2D transient viscoplastic model for dislocation generation of SiC by PVT method. In *Challenges in Mechanics of Time Dependent Materials*; Springer: Berlin, Germany, 2017; Volume 2.
21. Lin, M.; Chen, Q.; Tsai, C. Time-Dependent viscoplastic model for dislocation generation during the cooling process in the silicon ingot. In *Challenges in Mechanics of Time Dependent Materials*; Springer: Berlin, Germany, 2016; Volume 2.
22. Zhu, X.A.; Tsai, C.T. Finite element simulation of dislocation generation in doped and undoped GaAs single crystals grown from the melt. *Comput. Mater. Sci.* **2004**, *29*, 334–352. [[CrossRef](#)]
23. Zhao, W.; Liu, L.; Sun, L.; Geng, A. Quality evaluation of multi-crystalline silicon ingots produced in a directional solidification furnace with different theories. *J. Cryst. Growth* **2014**, *401*, 296–301. [[CrossRef](#)]



© 2019 by the authors. Licensee MDPI, Basel, Switzerland. This article is an open access article distributed under the terms and conditions of the Creative Commons Attribution (CC BY) license (<http://creativecommons.org/licenses/by/4.0/>).